Published in final edited form as:
NMR Biomed. 2011 June ; 24(5): 452–457. doi:10.1002/nbm.1610.

Preliminary observations of increased diffusional kurtosis in human brain following recent cerebral infarction

Jens H. Jensen[a,b,*], **Maria F. Falangola**[a,c], **Caixia Hu**[a,c], **Ali Tabesh**[a], **Otto Rapalino**[d], **Calvin Lo**[a], and **Joseph A. Helpern**[a,b,c,e]

[a]Center for Biomedical Imaging, Department of Radiology, New York University School of Medicine, New York, NY, USA

[b]Department of Physiology and Neuroscience, New York University School of Medicine, New York, NY, USA

[c]Center for Advanced Brain Imaging, Nathan S. Kline Institute for Psychiatric Research, Orangeburg, NY, USA

[d]Neuroradiology Division, Department of Radiology, Massachusetts General Hospital, Boston, MA, USA

[e]Department of Psychiatry, New York University School of Medicine, New York, NY, USA

Abstract

By application of the MRI method of diffusional kurtosis imaging, a substantially increased diffusional kurtosis was observed within the cerebral ischemic lesions of three stroke subjects, 13–26 h following the onset of symptoms. This increase is interpreted as probably reflecting a higher degree of diffusional heterogeneity in the lesions when compared with normal-appearing contralateral tissue. In addition, for two of the subjects with white matter infarcts, the increase had a strong fiber tract orientational dependence. It is proposed that this effect is consistent with a large drop in the intra-axonal diffusivity, possibly related to either axonal varicosities or alterations associated with the endoplasmic reticulum.

Keywords

ischemia; stroke; diffusion; brain; kurtosis; DKI; DTI; MRI

INTRODUCTION

In patients with acute and early subacute stroke, ischemia typically results in brain lesions in which the water self-diffusion coefficient, as measured by diffusion-weighted MRI, is reduced by approximately 50% relative to normal values (1). For this reason, diffusion-weighted MRI is widely used as a clinical tool to assess the extent of injury (2,3). The underlying mechanisms for the decreased diffusion are still not fully understood, although cell swelling (4–6), changes in cell membrane permeability (7,8), decreased cytoplasmic streaming (9,10) and increased intra-cellular viscosity (9,11) have been proposed.

*Correspondence to: J. H. Jensen, Department of Radiology, New York University School of Medicine, 660 First Avenue, 4th Floor, New York, NY 10016-3295, USA. jj33@nyu.edu.

A retrospective analysis by Jensen and Helpern (12) of animal data obtained by Pfeuffer *et al.* (13) has suggested that another diffusion metric, the diffusional kurtosis, may be increased substantially by ischemia. This was confirmed for human stroke patients in two recent preliminary studies (14,15). Diffusional kurtosis is a measure of the non-Gaussian nature of the diffusion displacement probability distribution, and is closely associated with diffusional heterogeneity (12,16,17).

In this study, the diffusional kurtosis and related metrics were obtained for three subjects with focal ischemia confined to a single hemisphere, using a diffusion-weighted imaging approach, referred to as diffusional kurtosis imaging (DKI) (16–18). Our analysis differed from previous DKI stroke work in that diffusional kurtosis was calculated for directions both parallel and perpendicular to the diffusion tensor eigenvector with the largest eigenvalue. In white matter, this eigenvector tends to be oriented in the same direction as the axon bundles. We also emphasize that the previous studies of refs. (14) and (15) were published only as conference abstracts, and therefore this report is, to the best of our knowledge, the first detailed description of diffusional kurtosis changes observed in human stroke patients.

Diffusional kurtosis changes in ischemic lesions were calculated relative to values for the contralateral, normal-appearing hemispheres. These were compared with alterations in more conventional diffusion coefficient metrics, such as the mean diffusivity (MD) and fractional anisotropy (FA), and interpreted in terms of known or plausible changes in tissue microstructure associated with ischemia. By more fully characterizing the effect of ischemia on water diffusion in brain, our results may help to constrain mechanistic models for ischemia-induced diffusion changes.

METHODS

Subjects

Three subjects presenting with focal cerebral ischemia were identified and studied under a protocol approved by the Institutional Review Board of the New York University Langone Medical Center. Subject 1 was a 75-year-old woman who received an MRI scan approximately 26 h following the acute onset of focal neurologic symptoms. Computed tomography images (25 h after onset and 1 h prior to MRI) showed an area of hypodensity in the region of the left frontal operculum, extending to the left anterior insular cortex, consistent with infarction. Subject 2 was a 49-year-old man who was scanned approximately 24 h following onset. Diffusion-weighted images showed an area of reduced diffusion in the left thalamus and posterior limb of the left internal capsule, compatible with infarction. Subject 3 was a 61-year-old man who was scanned approximately 13 h following onset. Diffusion-weighted images showed an area of reduced diffusion in the left parietal lobe, compatible with a left parietal infarction. Several smaller foci of infarction were seen in the left posterior corona radiata, and mild to moderate ischemic microvascular white matter disease was present.

Imaging

All subjects were scanned on an Avanto 1.5-T MRI scanner (Siemens Healthcare, Erlangen, Germany) using a vendor-supplied, diffusion-weighted, echo planar imaging sequence. A twice-refocused, diffusion-weighted sequence was used to reduce eddy currents. For Subject 1, three b values were used (0, 1000 and 2000 s/mm^2), with other imaging parameters as follows: number of diffusion directions, 30; slice thickness, 5 mm; slice gap, 0; number of slices, 30; TE = 96 ms; TR = 4500 ms; in-plane resolution, 2.6 mm × 2.6 mm; field of view, 229 mm × 208 mm; bandwidth, 1355 Hz/pixel. For Subjects 2 and 3, six b values were used (0, 500, 1000, 1500, 2000 and 2500 s/mm^2), with other imaging parameters as follows:

number of diffusion directions, 30; slice thickness, 5 mm; slice gap, 0; number of slices, 9; TE = 104 ms; TR = 1500 ms; in-plane resolution, 2 mm × 2 mm; field of view, 256 mm × 256 mm; bandwidth, 1345 Hz/pixel. For all subjects, three-quarter partial Fourier encoding, together with parallel imaging (acceleration factor, 2), was employed, and nine additional $b = 0$ images were acquired for better signal averaging.

Analysis

A DKI dataset differs from a diffusion tensor imaging (DTI) dataset in requiring at least three b values, rather than two, and at least 15 diffusion directions, rather than six (16–18). In addition, the maximum b values for DKI should be somewhat higher than for DTI; for brain, this means that the maximum b value for DKI should be about 2000–3000 s/mm^2. It is the use of these higher b values that sensitizes the diffusion-weighted signal to diffusional non-Gaussianity.

The post-processing of the data was performed in a manner similar to that previously described (17,18), using in-house software programmed in Matlab (The MathWorks, Inc., Natick, MA, USA). This differs from a conventional DTI analysis in that the diffusion-weighted signal intensity for a given diffusion direction as a function of the b value, S(b), is fitted to:

$$S(b) = S(0)\exp\left(-bD + \frac{1}{6}b^2D^2K\right) \quad [1]$$

where D is the apparent diffusion coefficient and K is the apparent diffusional kurtosis. From the values for D and K in each direction, both the standard rank two diffusion tensor and a rank four kurtosis tensor are constructed. With these two tensors, a number of diffusion metrics may be determined.

For this study, we considered the DTI metrics of MD, FA, axial diffusivity ($D_\parallel$) and radial diffusivity ($D_\perp$), as well as the additional DKI metrics of mean kurtosis (MK), axial kurtosis ($K_\parallel$) and radial kurtosis ($K_\perp$). MK is defined as the average of the kurtosis over all possible diffusion directions. $K_\parallel$ is defined, in analogy with $D_\parallel$, as the kurtosis in the direction of the diffusion tensor eigenvector with the largest diffusion eigenvalue, and $K_\perp$ is defined as the average of the kurtosis over all directions perpendicular to the diffusion eigenvector with the largest eigenvalue. In white matter, the axial direction is typically aligned with the axon bundles. Thus, $D_\parallel$ and $K_\parallel$ correspond to the diffusion coefficient and kurtosis along the axons, whereas $D_\perp$ and $K_\perp$ correspond to the diffusion coefficient and kurtosis averaged over all directions perpendicular to the axons. The notions of $K_\parallel$ and $K_\perp$ were first introduced by Hui *et al.* (19), although our definition for $K_\perp$ is not identical to theirs, as explained in ref. (17). All these seven metrics were derived from a single diffusion-weighted imaging dataset.

Parametric maps were calculated for all the above diffusion metrics. All images for a given subject were coregistered to correct for movement prior to map construction. For each subject, a single slice was selected that best showed the ischemic lesion. Rectangular regions of interest (ROIs) were defined for each lesion using the MD and MK maps, and ROIs of the same size were located on a corresponding area of the normal-appearing contralateral hemisphere (Figs 2 and 3, see `Results' section). The ROIs for the lesions were chosen to lie within the cores, as identified by the MD and MK maps, and the positioning of the contralateral ROIs was confirmed by a neuropathologist (MFF). For Subject 1, the ROI contained 36 voxels and represented a total volume of 1217 mm^3, and, for Subjects 2 and 3, the ROI contained 12 voxels and represented a total volume of 240 mm^3. Final values for

the seven diffusion metrics were obtained by averaging the maps over the ROIs. The percentage changes caused by ischemia were calculated using the formula:

$$\text{Percentage change} = 100 \times \frac{X_{\text{ischemia}} - X_{\text{contralateral}}}{X_{\text{contralateral}}} \quad [2]$$

where X represents an averaged diffusion metric.

RESULTS

The T_2-weighted images obtained from the diffusion-weighted sequence with $b = 0$ are shown in Fig. 1. The red arrows indicate the regions used for the analysis of the diffusion metrics. Hyperintensity suggestive of edema is apparent, although the areas of hyperintensity do not necessarily coincide with the ROIs used for the analysis, as these were based on the MD and MK maps.

Parametric maps of the conventional DTI diffusion metrics for the three subjects are shown in Fig. 2. The MD within the affected regions is hypointense relative to the contralateral side, as expected for acute to subacute focal ischemic lesions (1). Maps of additional metrics associated with diffusional kurtosis are shown in Fig. 3. The MK of the lesions is hyperintense, consistent with the suggestion of Jensen and Helpern (12).

The average values for each of the ROIs are shown in Fig. 4, together with the percentage changes averaged over all three subjects. The MD, $D_{\parallel}$ and $D_{\perp}$ were reduced in the ischemic regions by 52±6%, 59±2% and 43±11%, respectively (average for three subjects±standard error). This indicates that diffusion in both the axial and radial directions in the ischemic regions is more restricted than in the contralateral regions, with the drop in the axial direction being somewhat larger.

The average FA decreased by 25±24%, although FA for Subject 1 actually increased by 22%. It should be noted that the contralateral FA values for Subjects 2 and 3 (0.61 and 0.49) were substantially higher than for Subject 1 (0.28). This suggests that the ROIs for Subjects 2 and 3 were predominantly composed of axonal bundles with a high degree of directional orientation, whereas the ROI for Subject 1 contained a more isotropic distribution of crossing bundles and/or gray matter.

The MK, $K_{\parallel}$ and $K_{\perp}$ were increased in ischemic regions by 84±25%, 120±21% and 49±41%, respectively. This indicates that diffusion in ischemic regions, is more non-Gaussian, with this effect being much more pronounced in the axial direction than in the radial direction. Indeed, for Subjects 2 and 3, there were only very small increases in $K_{\perp}$ (3% and 12%), but there were large increases in $K_{\parallel}$ for all three subjects.

DISCUSSION

Our results show MD reductions of about 40–60% and MK increases of about 50–150% as a result of ischemia, studied at 13–26 h after symptom onset. The MD reductions were comparable with those typically observed in acute to subacute cerebral ischemia (1), and the MK increases were comparable with those estimated previously for rat brain (12). In addition, the diffusional changes were found to be greater, particularly for the kurtosis, in the axial direction than in the radial direction.

The increase in kurtosis probably reflects an increase in diffusional heterogeneity (17). This connection can be made precise for multiple-compartment models by the formula (16):

$$K = 3\frac{\delta^2 D}{D^2} \quad [3]$$

where $\delta^2 D$ is the variance of the compartmental diffusivities and Gaussian diffusion is assumed within each compartment. Thus, the kurtosis is equal to three times the square of the coefficient of variation for the diffusivities. Of course, multiple-compartment models may be too simple to accurately describe real brain tissue, but the existence of well-defined tissue compartments, such as the intracellular and extracellular spaces, makes them plausible idealizations.

The most striking results of this study were the large increases in $K_\parallel$ in conjunction with only small increases in $K_\perp$ for Subjects 2 and 3. Interestingly, the high contralateral FA values for these two subjects suggest that the ischemic regions were mainly in white matter with strongly oriented axon bundles. One explanation for this observation would be a large change in the intra-axonal diffusivity. This could increase $K_\parallel$ by increasing the diffusional heterogeneity in the axial direction. However, a change in the intra-axonal diffusivity would not necessarily change the radial diffusivity of the axonal compartment, since, for the diffusion times used in this experiment (~ 40 ms), the small axonal diameter (~ 1 μm) and low water permeability for myelinated axonal membranes mean that the effective radial diffusivity for this compartment will be close to zero, regardless of the value of the intra-axonal diffusivity.

At least two types of mechanism can be proposed for an ischemia-induced change in the intra-axonal diffusivity. First, it is known that ischemia (as well as other types of brain injury) can cause axonal varicosities (20,21). These bead-like swellings could act as diffusion dead-space microdomains (22,23), thereby lowering the along-axis diffusivity. Second, ischemia could alter the endoplasmic reticulum (the principal intra-axonal diffusion barriers) in such a manner as to decrease the intra-axonal diffusivity. This alteration could conceivably be a change in geometrical arrangement, perhaps caused by cytoskeletal breakdown (24), a decrease in permeability or an accumulation of unfolded proteins within the lumen of the endoplasmic reticulum (25). For either of these mechanisms, the increase in $K_\parallel$ is attributed to a sharp decrease in the axial diffusivity for the axonal compartment, but little change in the radial axonal diffusivity, which is forced to be very low by the axonal membranes and hence insensitive to the intra-axonal diffusivity. It should be noted that independent evidence supports a view that different processes are responsible for ischemic damage in white and gray matter (26).

Both of these mechanisms would also contribute to the observed decrease in $D_\parallel$, but not to the decrease in $D_\perp$, which could then be attributed to additional mechanisms (e.g. glial cell swelling). The fact that the decreases for Subjects 2 and 3 in $D_\parallel$ (63% and 55%) are significantly larger than for $D_\perp$ (40% and 26%) is consistent with this hypothesis. The decrease in FA for these two subjects (38% and 58%) also fits with a decrease in the axial diffusivity for the axonal compartment. Similar orientation-dependent diffusion coefficient changes in white matter have been reported previously by Tamura *et al.* (27).

These results and potential explanations are preliminary, in that only three subjects have been studied and only two of these had lesions in regions likely to have a high proportion of strongly oriented axon bundles. In addition, our calculated changes in diffusion metrics were based on contralateral ROIs, which may yield imperfect reference values. Therefore, further experiments are necessary to assess the generalizability of our conclusions.

Our results are consistent with the study of five stroke subjects by Helpern *et al.* (15), who observed similar large regions with elevated MK values. However, that study also reported

regions with decreased MK within some lesions. Lätt *et al.* (14), in a study of nine stroke subjects, measured (for a diffusion time of 60 ms) a kurtosis increase in white matter of 84%, but of only 6% in gray matter. In addition, they found a dependence of the kurtosis on the diffusion time. This diversity of results may reflect intersubject heterogeneity, as well as the complexity of ischemia-induced diffusion effects. An important outstanding question is how strongly the kurtosis changes depend on the time from symptom onset.

CONCLUSIONS

We have observed substantial increases in MK within ischemic lesions for three stroke patients. The magnitudes of the increases match well the predictions based on animal data (12), and are generally consistent with previous human studies (14,15). For the first time, we have determined the changes in $K_{\parallel}$ and $K_{\perp}$ for human focal cerebral infarction. For lesions with strongly oriented axon bundles (i.e. large contralateral FA values), the change in $K_{\parallel}$ was much greater than that in $K_{\perp}$, suggestive of a large decrease in the intra-axonal diffusivity. More broadly, our study illustrates how the application of DKI to the investigation of ischemic stroke can lead to a better characterization of the associated and still not fully understood water diffusion changes.

Acknowledgments

We thank Dr Steven Levine for helpful comments. This work was supported by the National Institutes of Health (contract/grant numbers 1R01AG027852 and 1R01EB007656) and the Litwin Foundation for Alzheimer's Research.

Abbreviations used

DKI	diffusional kurtosis imaging
DTI	diffusion tensor imaging
FA	fractional anisotropy
MD	mean diffusivity
MK	mean kurtosis
ROI	region of interest

REFERENCES

1. Schlaug G, Siewert B, Benfield A, Edelman RR, Warach S. Time course of the apparent diffusion coefficient (ADC) abnormality in human stroke. Neurology. 1997; 49:113–119. [PubMed: 9222178]
2. Lutsep HL, Albers GW, DeCrespigny A, Kamat GN, Marks MP, Moseley ME. Clinical utility of diffusion-weighted magnetic resonance imaging in the assessment of ischemic stroke. Ann. Neurol. 1997; 41:574–580. [PubMed: 9153518]
3. Schaefer PW, Grant PE, Gonzalez RG. Diffusion-weighted MR imaging of the brain. Radiology. 2000; 217:331–345. [PubMed: 11058626]
4. Benveniste H, Hedlund LW, Johnson GA. Mechanism of detection of acute cerebral ischemia in rats by diffusion-weighted magnetic resonance microscopy. Stroke. 1992; 23:746–754. [PubMed: 1374575]
5. Latour LL, Svoboda K, Mitra PP, Sotak CH. Time-dependent diffusion of water in a biological model system. Proc. Natl. Acad. Sci. USA. 1994; 91:1229–1233. [PubMed: 8108392]
6. Szafer A, Zhong J, Gore JC. Theoretical model for water diffusion in tissues. Magn. Reson. Med. 1995; 33:697–712. [PubMed: 7596275]

7. Helpern, JA.; Ordidge, RJ.; Knight, RA. The effect of cell membrane permeability on the apparent diffusion coefficient of water. Proceedings of the 11th Annual Meeting of ISMRM; Berlin, Germany. 1992. p. 201
8. Lee JH, Springer CS. Effects of equilibrium exchange on diffusion-weighted NMR signals: the diffusigraphic `shutter-speed'. Magn. Reson. Med. 2003; 49:450–458. [PubMed: 12594747]
9. Dijkhuizen RM, de Graaf RA, Tulleken KA, Nicolay K. Changes in the diffusion of water and intracellular metabolites after excitotoxic injury and global ischemia in neonatal rat brain. J. Cereb. Blood Flow Metab. 1999; 19:341–349. [PubMed: 10078886]
10. Silva MD, Omae T, Helmer KG, Li F, Fisher M, Sotak CH. Separating changes in the intra- and extracellular water apparent diffusion coefficient following focal cerebral ischemia in the rat brain. Magn. Reson. Med. 2002; 48:826–837. [PubMed: 12417997]
11. van Pul C, Jennekens W, Nicolay K, Kopinga K, Wijn PF. Ischemia-induced ADC changes are larger than osmotically-induced ADC changes in a neonatal rat hippocampus model. Magn. Reson. Med. 2005; 53:348–355. [PubMed: 15678540]
12. Jensen, JH.; Helpern, JA. Quantifying non-Gaussian water diffusion by means of pulsed-field-gradient MRI. Proceedings of the 11th Annual Meeting of ISMRM; Toronto, QC, Canada. 2003. p. 2154
13. Pfeuffer J, Provencher SW, Gruetter R. Water diffusion in rat brain in vivo as detected at very large b values is multicompartmental. MAGMA. 1999; 8:98–108. [PubMed: 10456372]
14. Lätt, J.; van Westen, D.; Nilsson, M.; Wirestam, R.; Ståhlberg, F.; Holtås, S.; Brockstedt, S. Diffusion time dependent kurtosis maps visualize ischemic lesions in stroke patients. Proceedings of the 17th Annual Meeting of ISMRM; Honolulu, HI, USA. 2009. p. 40
15. Helpern, JA.; Lo, C.; Hu, C.; Falangola, MF.; Rapalino, O.; Jensen, JH. Diffusional kurtosis imaging in acute human stroke. Proceedings of the 17th Annual Meeting of ISMRM; Honolulu, HI, USA. 2009. p. 3493
16. Jensen JH, Helpern JA, Ramani A, Lu H, Kaczynski K. Diffusional kurtosis imaging: the quantification of non-Gaussian water diffusion by means of magnetic resonance imaging. Magn. Reson. Med. 2005; 53:1432–1440. [PubMed: 15906300]
17. Jensen JH, Helpern JA. MRI quantification of non-Gaussian water diffusion by kurtosis analysis. NMR Biomed. 2010; 23:698–710. [PubMed: 20632416]
18. Lu H, Jensen JH, Ramani A, Helpern JA. Three-dimensional characterization of non-Gaussian water diffusion in humans using diffusion kurtosis imaging. NMR Biomed. 2006; 19:236–247. [PubMed: 16521095]
19. Hui ES, Cheung MM, Qi L, Wu EX. Towards better MR characterization of neural tissues using directional diffusion kurtosis analysis. Neuroimage. 2008; 42:122–134. [PubMed: 18524628]
20. Hou ST, Jiang SX, Aylsworth A, Ferguson G, Slinn J, Hu H, Leung T, Kappler J, Kaibuchi K. CaMKII phosphorylates collapsin response mediator protein 2 and modulates axonal damage during glutamate excitotoxicity. J. Neurochem. 2009; 111:870–881. [PubMed: 19735446]
21. Takeuchi H, Mizuno T, Zhang G, Wang J, Kawanokuchi J, Kuno R, Suzumura A. Neuritic beading induced by activated microglia is an early feature of neuronal dysfunction toward neuronal death by inhibition of mitochondrial respiration and axonal transport. J. Biol. Chem. 2005; 280:10, 444–10, 454.
22. Tao A, Tao L, Nicholson C. Cell cavities increase tortuosity in brain extracellular space. J. Theor. Biol. 2005; 234:525–536. [PubMed: 15808873]
23. Budde, MD.; Frank, JA. Neurite beading is sufficient to decrease the apparent diffusion coefficient following ischemic stroke. Proceedings of the 18th Annual Meeting of ISMRM; Stockholm, Sweden. 2010. p. 299
24. Dewar D, Dawson DA. Changes of cytoskeletal protein immunostaining in myelinated fibre tracts after focal cerebral ischaemia in the rat. Acta Neuropathol. 1997; 93:71–77. [PubMed: 9006659]
25. Oida Y, Shimazawa M, Imaizumi K, Hara H. Involvement of endoplasmic reticulum stress in the neuronal death induced by transient forebrain ischemia in gerbil. Neuroscience. 2008; 151:111–119. [PubMed: 18082969]
26. Verkhratsky A. Physiology and pathophysiology of the calcium store in the endoplasmic reticulum of neurons. Physiol. Rev. 2005; 85:201–279. [PubMed: 15618481]

27. Tamura H, Kurihara N, Machida Y, Nishino A, Shimosegawa E. How does water diffusion in human white matter change following ischemic stroke? Magn. Reson. Med. Sci. 2009; 8:121–134. [PubMed: 19783875]

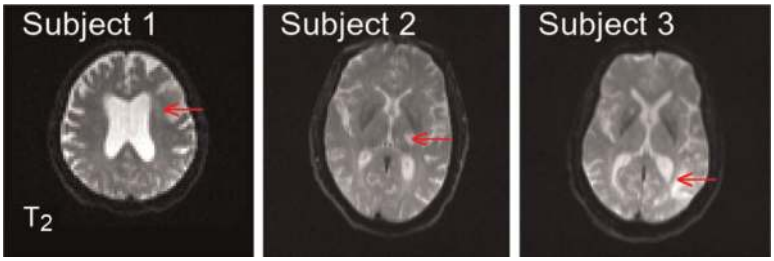

Figure 1.
T_2-weighted ($b = 0$) images for a single slice from each of the three subjects. The red arrows indicate the lesion areas used for the analysis of the diffusion metrics.

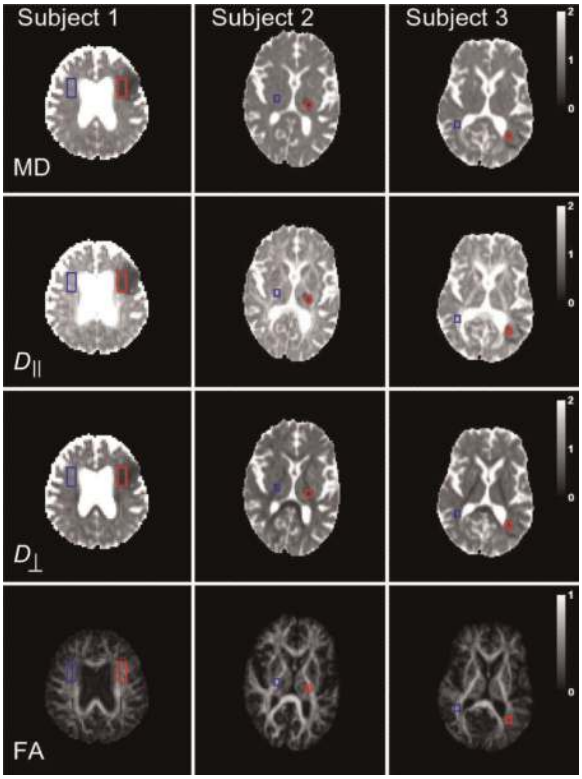

Figure 2.
Parametric maps of the four conventional diffusion metrics for the three subjects. The regions of interest (ROIs) for the ischemic lesions are shown in red, and the contralateral ROIs are shown in blue. The calibration bars for the diffusivities are in units of $\mu m^2/ms$, whereas those for the fractional anisotropy (FA) are dimensionless. $D_{\perp}$, radial diffusivity; $D_{||}$, axial diffusivity; MD, mean diffusivity.

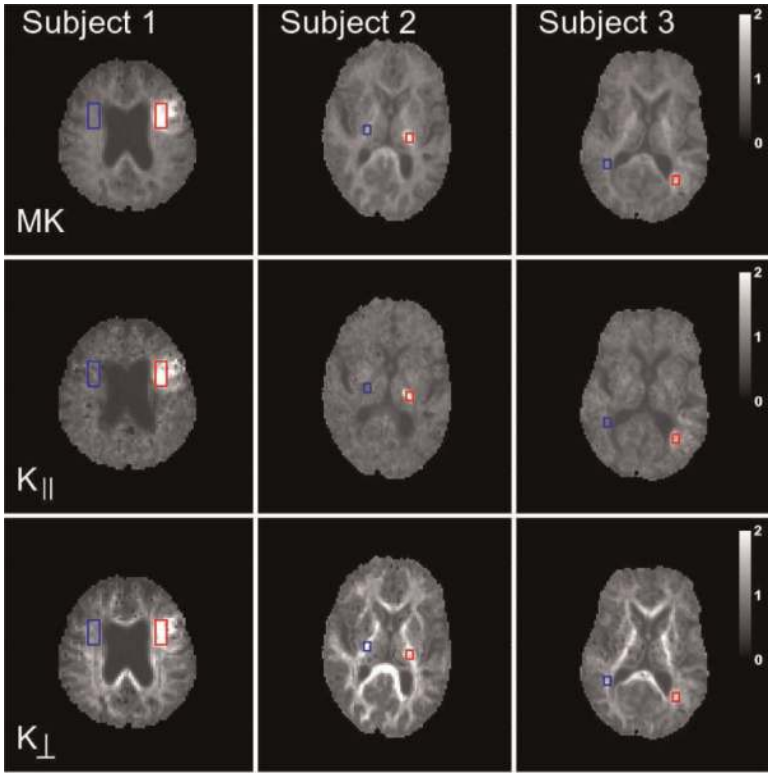

Figure 3.
Parametric maps of the three diffusional kurtosis metrics for the same slices as shown in Fig. 2. All metrics in Figs 2 and 3 for a given subject are derived from a single diffusional kurtosis imaging (DKI) dataset. Note the relatively larger differences between the ischemic and contralateral sides for the axial kurtosis ($K_{\parallel}$) relative to the radial kurtosis ($K_{\perp}$) for Subjects 2 and 3. The calibration bars for the kurtoses are dimensionless. MK, mean kurtosis.

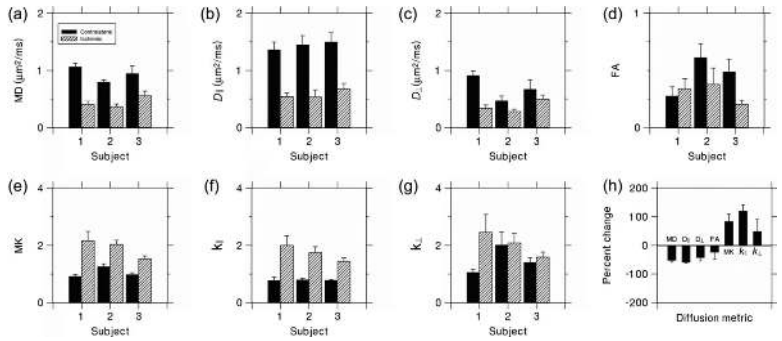

Figure 4.

(a–g) Values of the diffusion metrics averaged over the regions of interest (ROIs). The error bars indicate the standard deviations. Note the particularly large differences between the contralateral and ischemic ROIs for $D_{\parallel}$ and $K_{\parallel}$. (h) Percentage changes for the diffusion metrics in the ischemic ROI relative to the contralateral ROI, averaged over all three subjects. The error bars indicate the standard errors. $D_{\perp}$, radial diffusivity; $D_{\parallel}$, axial diffusivity; FA, fractional anisotropy; $K_{\perp}$, radial kurtosis; $K_{\parallel}$, axial kurtosis; MD, mean diffusivity; MK, mean kurtosis.